An instrument to control parallel plate separation for nanoscale flow control

J. White[a)]
Department of Mechanical Engineering, Massachusetts Institute of Technology, Cambridge, Massachusetts 02139

H. Ma
Department of Media Arts and Sciences, Massachusetts Institute of Technology, Cambridge, Massachusetts 02139

J. Lang
Department of Electrical Engineering, Massachusetts Institute of Technology, Cambridge, Massachusetts 02139

A. Slocum
Department of Mechanical Engineering, Massachusetts Institute of Technology, Cambridge, Massachusetts 02139

(Received 22 July 2003; accepted 1 September 2003)

The handling of extremely small samples of gases and liquids has long been a subject of research among biologists, chemists, and engineers. A few scientific instruments, notably the surface force apparatus, have been used extensively to investigate very short-range molecular phenomena. This article describes the design, fabrication, and characterization of an easily manufactured, gas and liquid flow control device called the *Nanogate*. The Nanogate controls liquid flows under very high planar confinement, wherein the liquid film is, in one dimension, on the scale of nanometers, but is on the scale of hundreds of microns in its other dimensions. The liquid film is confined between a silica (Pyrex) surface with a typical roughness of Ra≈6 nm and a gold-covered silicon surface with a typical roughness of Ra≈2 nm. During the manufacturing process, the Pyrex flows and conforms to the gold-covered silicon surface, improving the mating properties of the two surfaces. The fluid film thickness can be controlled within 2 Å, from sub-10 nm up to 1 μm. Control of helium gas flow rates in the 10^{-9} atm cm^3/s range, and sub-nl/s flow rates of water and methanol have been predicted and experimentally verified. © *2003 American Institute of Physics.*
[DOI: 10.1063/1.1621066]

I. INTRODUCTION

The physics of fluid flows confined to a channel of molecular dimensions, which are understood to be on the order of nanometers, are sometimes substantially altered from what is observed in continuum systems. For example, in the case of a gaseous mixture flowing in a sufficiently narrow channel, molecules of different molecular weights flow at different rates. With simple liquids confined between mica sheets separated by less than ten molecular dimensions, solidification, wherein the liquid viscosity increases beyond its bulk value, has been observed using the surface force apparatus.[1,2] Slip flow, where the fluid viscosity appears to decrease below its bulk value, has been observed, again with the surface force apparatus, in nondegassed liquids (both polar and nonpolar) between nonwetting mica surfaces, even at relatively large separation distances of 50 nm.[3] These effects were observed to disappear with increasing surface roughness.[4] However, the surface force apparatus is not necessarily an ideal mechanism for studying fluid flows since it is an indirect approach where the viscosity is inferred from the measurement of surface forces acting over an area that is not precisely defined. In addition, ensuring some liquids have no dissolved gas can be difficult in an open environment. An ideal apparatus for verifying these results would thus allow direct control of the plate separation, a well-defined interaction area, and a direct measurement of pressure-driven fluid flowrate.

In addition, with a long, narrow channel of sufficiently small dimensions, and appropriate surface chemistry, one can reasonably conceive of excluding particles based solely on their size. By making the channel height adjustable, a wide range of molecule sizes could be filtered without the loss of larger particles that is characteristic of a conventional porous filter. More generally, one could conceive of mechanically filtering a solution of unknown composition, particle by particle, or introducing minute, well-controlled quantities of liquid or gas into a chemical or biological process. A mechanical filter that operated in this manner might have applications in processes such as drug discovery, where the manipulation of extremely small quantities of liquid is required. The design challenge is therefore to create an adjustable device that can confine liquid flows on nanometer (or subnanometer) length scales.

a)Electronic mail: jwhite@mit.edu

 © 2003 American Institute of Physics

Downloaded 11 Oct 2008 to 18.100.0.118. Redistribution subject to AIP license or copyright; see http://rsi.aip.org/rsi/copyright.jsp

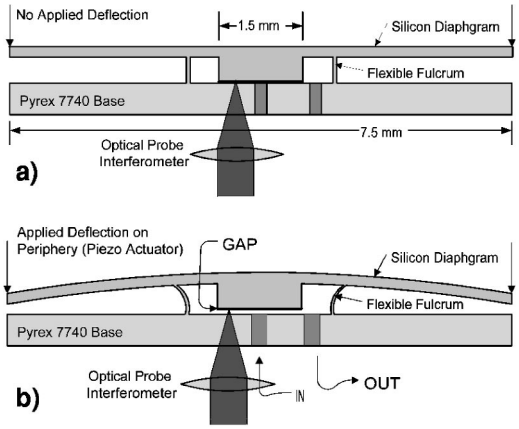

FIG. 1. Operation principle of the Nanogate showing (a) undeflected mode and (b) deflected mode.

A review of manufacturing processes[5] reveals that etched and machined surfaces typically have roughness on the order of hundreds of nanometers, and, similarly, feature contour and straightness on the order of microns. In comparison, flat surfaces, which are simple to manufacture, can have nanometer-scale flatness and surface finish and are readily obtained, for example, in the form of silicon wafers, glass wafers and optical flats. Mounting two polished surfaces in close proximity creates a very long, nanometer-high channel or aperture. Accordingly, a platform technology of ''surface finish mechanisms'' (SFMs) based on this principle was proposed by Slocum,[6] and this article describes research conducted to develop and test the design theory for this class of devices.

In a SFM, the minimum size of the aperture is limited only by the roughness and local bow and warp of the two opposed surfaces. In fact, as will be shown, certain manufacturing processes can cause the surfaces to conform to each other to the nanometer level, so initial bow and warp need not be of primary concern. As a result, in a nanometer-scale channel with a very large aspect ratio of height to length, (here, greater than 10^5), surface forces strongly influence the liquids that are flowing. Molecules inside the channel find

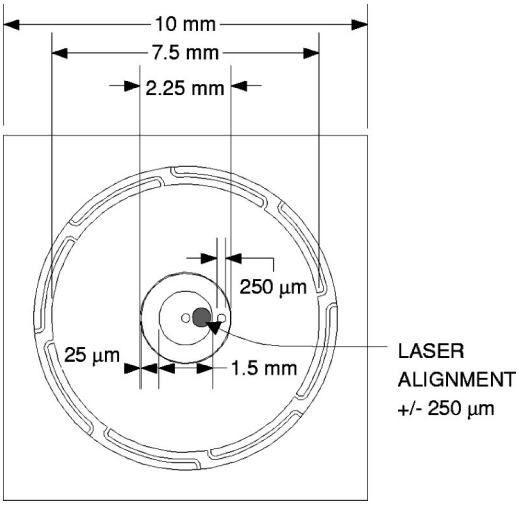

FIG. 2. Nanogate die dimensions.

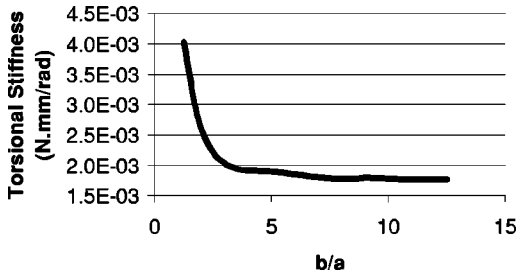

FIG. 3. Fulcrum stiffness vs height/thickness ratio (b/a).

themselves confined between two plates of essentially infinite extent in all directions. Therefore, the surface chemistry, planarity, and roughness can have a dominant effect on fluid flow properties.

The *Nanogate* is a fundamental embodiment of a SFM mechanism, as shown in the cross section in Figs. 1(a) and 1(b), where the axis of revolution is through the center of the device. It incorporates two parallel, polished, flat surfaces, several hundred microns in diameter, and a circular plate flexure and fulcrum mechanism to control their separation. The flexure structure acts as a mechanical transmission, and translates the (relatively) coarse motion of a macroscopic external actuator assembly into fine control over the separation of the central-plate region. The fulcrum's stiffness is far less than that of the circular plate flexure, and it also acts to isolate the flow region from the outside.

II. DESIGN

We have deliberately tried to use microelectromechanical systems (MEMS) technology where it gives the greatest

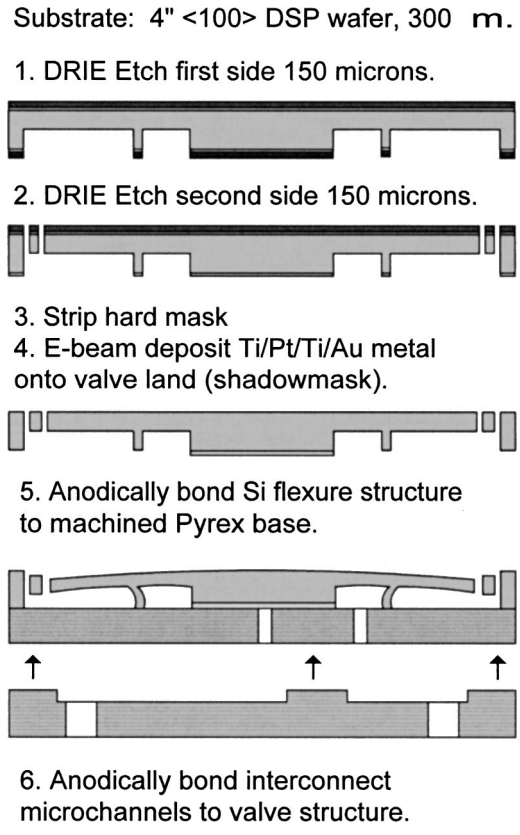

FIG. 4. Nanogate fabrication process.

Downloaded 11 Oct 2008 to 18.100.0.118. Redistribution subject to AIP license or copyright; see http://rsi.aip.org/rsi/copyright.jsp

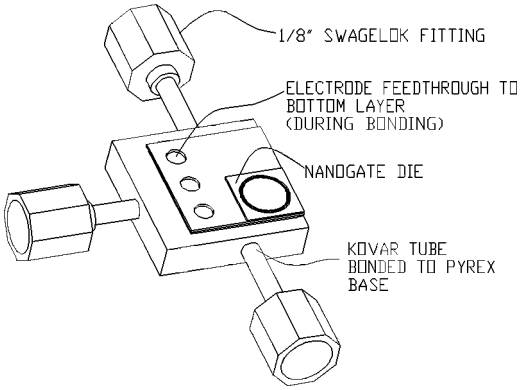

FIG. 5. Diagram of packaged Nanogate.

benefits, here in the production of very precise flexures and very highly polished surfaces. However, MEMS was not indicated for the high force precision actuators, nor is it necessarily most suitable for high-vacuum connectors and packaging. Therefore, the Nanogate is not a true MEMS device, but rather a nanosystem that incorporates both MEMS and conventional components. A true MEMS Nanogate would have the functions of actuation and metrology fully integrated into the parallel manufacturing process. The Nanogate is shown conceptually in a two-dimensional drawing in Fig. 1(a), where the axis of revolution is through the center of the device. The circular plate flexure diameter is 7.5 mm. The resulting lever and fulcrum mechanism has high mechanical impedance for prying the two surfaces apart. This has been fabricated as an etched silicon structure bonded to a Pyrex substrate. Deflections are applied to the periphery of the circular plate flexure, as shown in Fig. 1(b), causing separation of the top silicon and bottom Pyrex central surfaces.

The overall dimensions of the manufactured Nanogate are given in Fig. 2. Two parameters were of interest in designing this device. The first was the transmission ratio, which is the ratio of the deflection applied to the outer periphery of the circular plate flexure to the movement of the central boss (valve land). The second was the maximum aperture, limited by the stresses in the fulcrum. The deflection of the circular plate flexure can be readily calculated from plate theory,[7] neglecting the stiffness of the fulcrum (which, here, is 2% of the stiffness of the circular plate flexure), from which the transmission ratio, T, is found to be

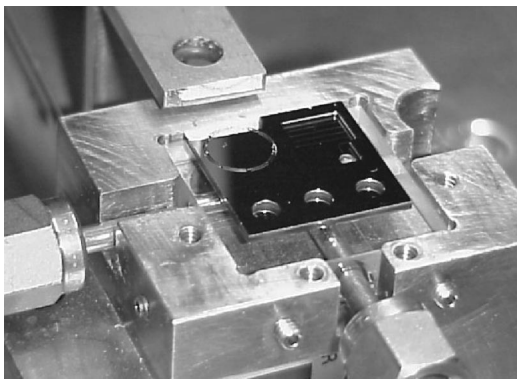

FIG. 6. Completed Nanogate die, mounted in fixture.

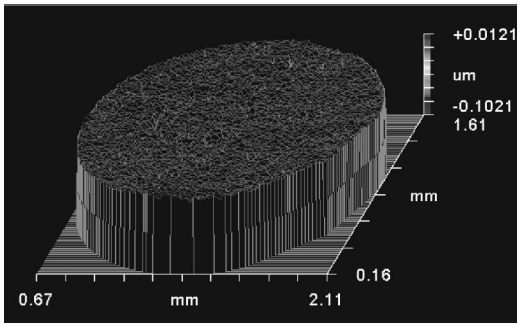

FIG. 7. Silicon surface measured by optical profilometry. Ra=2.1 nm.

$$T=\frac{w(r=a)}{w(r=0)}=16.9, \tag{1}$$

where w is the vertical deflection of the circular plate flexure, r is the radial position, and a is the outer radius of the circular plate flexure. The flexible fulcrum can be modeled as a semi-infinite cylindrical shell, provided that the ratio of height to thickness is greater than 3. Shorter fulcrums become stiffer, as shown in Fig. 3. The torsional stiffness (wrt. its fulcrum action) of the edge of the cylindrical shell is given by[8]

$$\tau=\frac{M_2}{\phi}=\lambda D, \tag{2}$$

where D is the plate stiffness of the shell

$$D=\frac{Et^3}{12(1-\nu^2)}, \tag{3}$$

E is Young's modulus (assumed 150 GPa for silicon), ν is Poisson's ratio (0.25 for silicon), t is the shell thickness (25 μm). λ is defined as

$$\lambda=\sqrt[4]{\frac{3(1-\nu^2)}{R^2t^2}}, \tag{4}$$

where R is the fulcrum radius (1.25 mm). The maximum stress in the fulcrum is at its attachment point to the circular plate flexure. At this point

$$\sigma_{\max}=\frac{2\lambda^3 DR}{t}\theta. \tag{5}$$

For the given geometry, assuming a maximum stress in the fulcrum of 1 GPa, the maximum deflection on the periphery

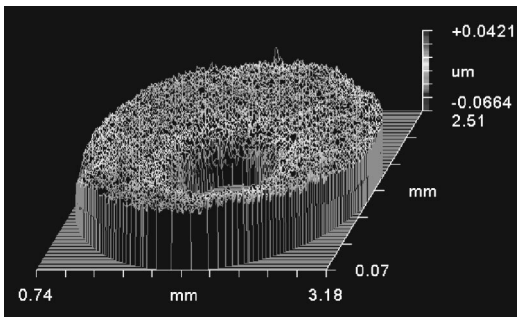

FIG. 8. Pyrex surface measured by optical profilometry. Ra=6.5 nm.

Downloaded 11 Oct 2008 to 18.100.0.118. Redistribution subject to AIP license or copyright; see http://rsi.aip.org/rsi/copyright.jsp

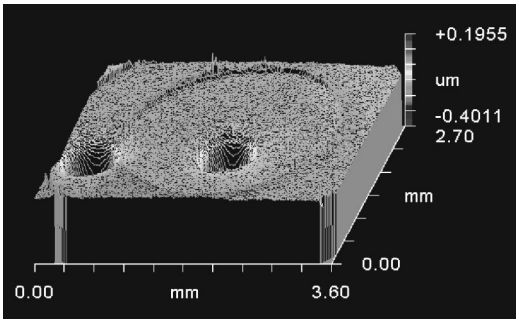

FIG. 9. Pyrex surface, deformed during the bonding process to match the silicon surface.

is 71 μm and the maximum deflection in the center of the valve land will be 4.2 μm, while the minimum central deflection is on the nanometer level from experimental testing. The Nanogate's open loop sensitivity to fluctuations in the input fluid pressure is calculated as 25 nm per 1 atm pressure change thus in the case of large inlet pressure fluctuations, high resolution position feedback may be employed to maintain the gap at its setpoint.

The lever-fulcrum action of the structure allows precise control of the gap opening. In our latest experiment, the opening and closing motion of the Nanogate has been measured in increments as small as 2 Å with constant inlet pressure. Furthermore, our results have shown that the gate does not experience pull-in or stiction instabilities during closing and opening in air. Two reasons have been put forward to explain why stiction is not an issue in this apparatus, while causing failures in many other MEMS devices. One is that gold and Pyrex glass have a very small chemical affinity and will not bond. The other is that the high stiffness of the system precludes us from seeing any stiction effects even if they exist. These results, combined with the flow results shown later, verify our fundamental design philosophy and indicate that we can have very stable control of the gap size. The first device built is a MEMS proportional fluid flow control valve.

III. FABRICATION

The high-precision wetted parts of the Nanogate are manufactured using conventional MEMS etching and bonding technologies. The flexure and fulcrum structure are etched from a silicon wafer using the Bosch deep reactive ion etch process.[9] The valve land is then coated with a thin layer of gold, and the finished silicon wafer is anodically bonded to a bare Pyrex wafer with machined interconnection holes. The gold layer (specifically, 20 nm Ti/100 nm Pt/20 nm Ti/100 nm Au) creates a selective bond by preventing bonding in the region where it is applied, and no additional release steps are required after bonding. The intervening layer of platinum prevents the gold from diffusing into the silicon during the bonding process and forming a eutectic AuSi layer, which will bond to glass. It is necessary to carefully monitor the thermal budget to avoid the formation of a gold–silicon eutectic during bonding. This parallel manufacturing approach, shown in Fig. 4, produces integrated nanoscale fluidic systems with virtually any fluidic interconnections. The ability to add electrical interconnections to this process will also be fundamental to integrating metrology in future generations.

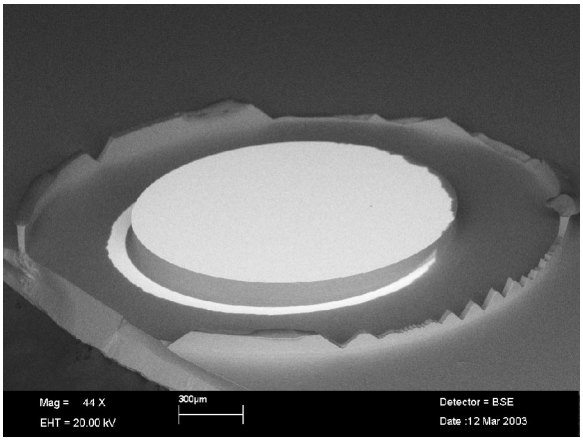

FIG. 11. SEM of silicon surface showing broken fulcrum.

The packaging of the Nanogate has proven fundamental to obtaining reliable experimental data. The Nanogate is packaged at the die level by anodically bonding the three-layer silicon and glass wafer stack to a polished, machined Pyrex die. Kovar tubes with Swagelok™ connectors are then bonded to the large Pyrex die, as shown in Figs. 5 and 6, using a leak sealant epoxy with minimal outgassing in high vacuum (Kurt Lesker KL-5, Kurt Lesker Inc., Clairton, PA). This large, rigid base provides standard connections to external apparatus such as syringe pumps, or high vacuum equipment. The package can be pumped down to 10^{-7} Torr, or

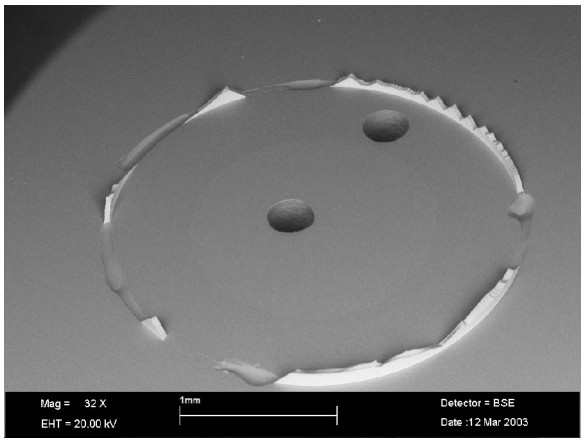

FIG. 10. SEM of Pyrex surface showing broken fulcrum.

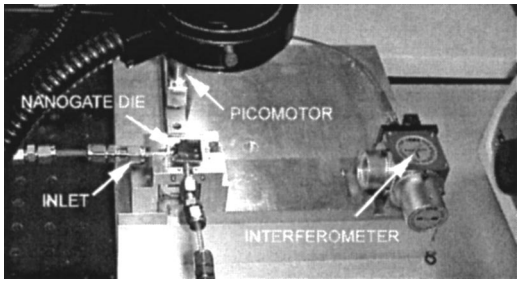

FIG. 12. Picture of Nanogate apparatus.

Downloaded 11 Oct 2008 to 18.100.0.118. Redistribution subject to AIP license or copyright; see http://rsi.aip.org/rsi/copyright.jsp

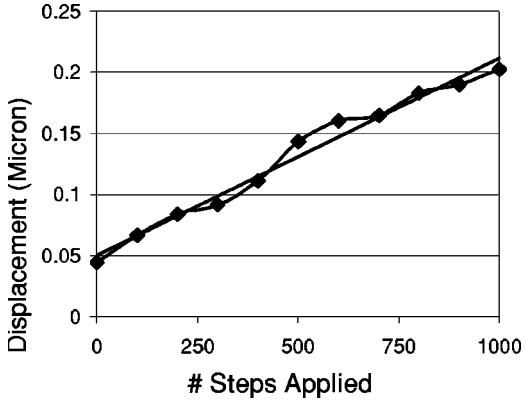

FIG. 13. Average change in position per step: 2 Å.

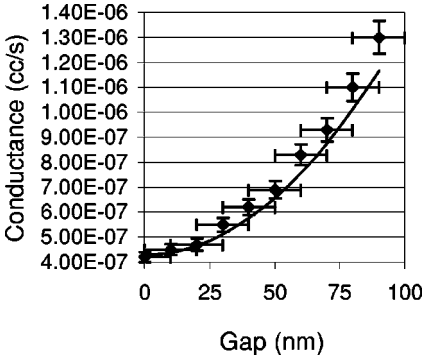

FIG. 14. Helium flow test (pressure drop: 6.35 psi into vacuum).

pressurized to over 100 psi without any adverse effects. Furthermore, it can be heated to 200 °C without damage.

Additional metrology studies on finished Nanogate dies indicated that the final surface roughness of the gold-coated silicon was Ra=2.1 nm, shown in Fig. 7, and the roughness of the Pyrex surface was Ra=6.5 nm, shown in Fig. 8. During the anodic bonding process (800 V at 325 °C until bonding current levels off, followed by 60 min cool-down) the Pyrex flows slightly, as shown in Fig. 9, causing the valve surfaces to mate conformally. The roughness of each surface is unchanged by the bonding process. This then relieves some of the requirements on the initial bow/warp of the mating surfaces, as the Pyrex will deform by approximately 40 nm to take the shape of the silicon boss.

A forensic examination of a Nanogate indicates that the bond between the fulcrum and the pyrex base is also very strong. Figures 10 and 11 show scanning electron microscopy (SEM) images of a forcibly disassembled Nanogate. It is evident that either the fulcrum breaks, or pieces of the Pyrex substrate are removed when the top and bottom layers are separated. This shows that the bond, and hence, the seal between the inner flow region and the outside world, is robust.

IV. ACTUATION, METROLOGY, AND MECHANICAL CHARACTERIZATION

The experimental apparatus consist of a Zygo ZMI 512 single-point laser interferometer with 2.4 nm resolution, for determining the deflection of the valve land, a piezoelectric stepper actuator, the New Focus Picomotor™, with approximately 3.5 nm step size (under load), Super Invar mounting fixtures and fluid handling equipment for each test case. A closeup of the basic apparatus is shown in Fig. 12.

The mechanical response of the Nanogate was calibrated using the Picomotor as the actuator and the Zygo optical probe for displacement metrology. The displacement of the valve land was thus measured directly. The average displacement of the valve land per applied Picomotor step was determined to be 2 Å, as inferred in Fig. 13 from measurements over a 150 nm excursion, corresponding to 750 applied Picomotor steps.

V. FLOW RESULTS: HELIUM

The flow of gases at atmospheric pressure in the Nanogate is described by Knudsen's equation for rareified gas flow[10]

$$U = \sqrt{\frac{RT}{M}}\frac{8}{3}\sqrt{2\pi}\frac{h^2}{\ln(r_2/r_1)}\ \mathrm{cm}^3/\mathrm{s}, \tag{6}$$

where M is the molecular mass, T is temperature, R is the ideal gas constant, h is the gap height, and r_2 and r_1 are the inner and outer radii of the flow channel. Helium leak tests were conducted using a Varian 979 helium leak tester, which uses a mass spectrometer to determine the leak rate, and has mass flow sensitivity of 10^{-10} atm cm^3/s. Helium leak tests were performed at room temperature (22 °C). The machine was self-calibrating, and before any tests were performed, the inlet was sealed, and the machine determined the baseline ("zero") leak rate. The outlet of the Nanogate valve was connected to the inlet of the helium leak tester using a 1/4 in.×24 in. flexible stainless steel tube with VCR-4 fittings on each end. The leak rate was then measured, at a given pressure drop, for a range of valve openings. The data obtained from our test artifact is summarized in Fig. 14. The minimum observed leak rate, for zero opening, was 4.1×10^{-7} atm cm^3/s; this quantity is expected to be a function of the artifact under test. However, the base line leak rate is also increased by gas leaks from the surrounding ambient air through the metal fittings and the package. After subtracting the baseline leak, the dependence of the flowrate on Nanogate displacement conforms very closely to what is predicted by Eq. (6). This would not be the case if an actual gap still existed, thus supporting the assertion that the base line leak was due to other sources and indicating the need for a better package. Fully open, however, the helium leak rate is greater than 1×10^{-3} atm cm^3/s, which exceeds the upper bound of the measurement capability of the helium leak tester. This indicates the nanogate can achieve over four decades of dynamic flow control. For comparison purposes, the capabilities of various similar flow control technologies are summarized in Table I.

Downloaded 11 Oct 2008 to 18.100.0.118. Redistribution subject to AIP license or copyright; see http://rsi.aip.org/rsi/copyright.jsp

TABLE I. Comparison of Nanogate to selected existing technologies.

Parameter	Nanogate	Yang *et al.*[a]	Varian[b] variable leak valve	Redwood microsystems[c] MFC
Minimum leak rate (He at 1 bar into vacuum)	2.7×10^{-7} atm cm^3/s	1×10^{-7} atm cm^3/s	$<10^{-10}$ atm cm^3/s	$\sim10^{-7}$ atm cm^3/s
Maximum flow rate (1 atm into vacuum)	$<10^{-3}$ atm cm^3/s	0.015 atm cm^3/s	$>10^{-3}$ atm cm^3/s	33.3 atm cm^3/s
Minimum controllable flow rate	10^{-9} atm cm^3/s	3×10^{-3} atm cm^3/s	10^{-10} atm cm^3/s	10^{-3} atm cm^3/s
Packaged size	1.0 in.×1.0 in.× 1.5 in. (w/o control electronics)	10 cm^3 (without drive electronics)	4.5 in.×4.5 in.× 2.5 in.	1.5 in.×4.5 in.×4.9 in. (with drive electronics)
Control method	Piezoelectric	Piezoelectric	Manual	Thermopneumatic
Valve position feedback	Yes	No	No	No
Particle-free operation	Yes	Indeterminate	No	Yes
Multiple valves per package?	Yes	Yes	No	Yes
"Hard" sealing materials (low He permeability)	Yes (gold on Pyrex)	Yes (silicon oxide on silicon oxide)	Yes (sapphire on metal)	No (elastomer seat)
Actuation mechanism	MEMS fulcrum and flexure plate	Piezoelectric actuator	Fine pitch screw thread/lever	Thermopneumatic fluid
Sealing mechanism	Conformal gold and Pyrex surfaces	Silicon oxide mating surfaces	Metal gasket against optically flat sapphire	Silicon boss against elastomer seat

[a]E. H. Yang *et al.*, "Normally-closed, leak-tight piezoelectric microvalve under ultra-high upstream pressure for integrated micropropulsion," MEMS 2003, Kyoto, 17–25 2003 Jan., pp. 80–83.
[b]Varian Inc., Lexington, MA.
[c]Redwood Microsystems, Menlo Park, CA.

VI. FLOW RESULTS: WATER AND METHANOL

Pressure driven flow tests were conducted with deionized water and methanol. In the Nanogate, liquid flow is entirely viscous, and governed by Poiseuille's equation for a toroidal geometry

$$Q=\frac{\pi h^3}{6\mu}\ln\left(\frac{r_2}{r_1}\right)\Delta P \quad \mathrm{m^3/s}, \tag{7}$$

where h is the gap height, μ is the viscosity, r_2 and r_1 are the outer and inner radii of the flow region, respectively, and ΔP is the pressure drop across the annulus. The inlet reservoir was connected to a pressurized nitrogen accumulator, thereby providing a constant inlet pressure to the valve. The outlet channel of the Nanogate, which is 45 mm long and has a constant cross section of 45 μm×100 μm, was directly observed with an optical microscope. Since the dimensions of the outlet channel were precisely measured in advance, the flow rate can be determined by observing the progress of the flow front's meniscus in an air-filled channel. The data for methanol is summarized in Fig. 15, which shows no departure from the expected (theoretical) prediction for methanol for channel heights down to 150 nm. The flow conditions for methanol were room temperature (22 °C) and a pressure drop of 20 psi. Liquid flow tests were also conducted with water for channel heights down to 80 nm, with a pressure drop of 40 psi, also at room temperature. These results are summarized in Fig. 16. The error bars on the position measurement

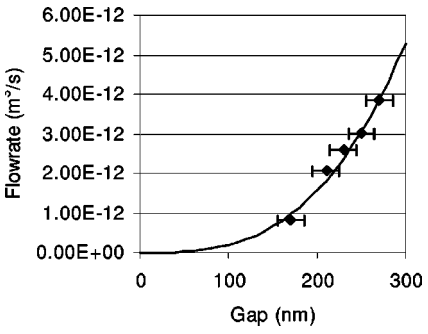

FIG. 15. Methanol flow test (pressure drop: 20 psi).

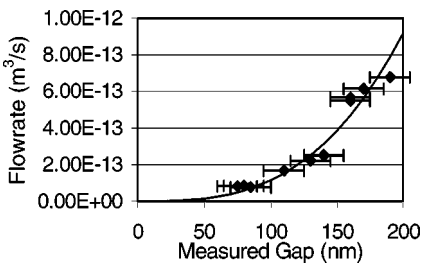

FIG. 16. Water flow test (pressure drop: 40 psi).

Downloaded 11 Oct 2008 to 18.100.0.118. Redistribution subject to AIP license or copyright; see http://rsi.aip.org/rsi/copyright.jsp

($\pm$15 nm) are the consequence of thermal fluctuations during the test interval. For very long measurement times (i.e., very small flow rates), thermal variances cause the interferometer reading to vary. Thus, thermal fluctuations limit the measurement time and the smallest flow rate that can be usefully observed in our simple system.

A final test was to evaluate the base line leak rate of water through the Nanogate when it was entirely closed. Water at a pressure of 40 psi was applied to the inlet for 7 days, but no flow could be observed. More elaborate tests, possibly using a mass spectrometer to detect any small leakage of liquid, would be required to confirm that the off-state flow rate was entirely zero.

VII. DISCUSSION

The no-slip boundary condition and the Navier–Stokes equations have been verified for water flowing past glass and gold surfaces separated by only 80 nm. Rarefied gas theory has been confirmed to describe atmospheric pressure gas flows in nanometer-scale channels. Immediate applications of the Nanogate are in ultrafine flow control and high complexity microfluidic systems. Further applications in gas chromatography and liquid separations have also been hypothesized but not yet demonstrated experimentally and are the subject of future work. More broadly, it is believed that the Nanogate can be regarded as a basic scientific instrument for research on the properties of highly confined, molecular-scale liquid and gas systems.

ACKNOWLEDGMENTS

This research was funded by NSF Grant No. DMI-0002934. J.W. gratefully acknowledges the support of the Hertz foundation. This article is based on the Ph.D thesis of the first author, which provides more details (see Ref. 11). Funds were also provided by the Deshpande Center for Technological Innovation.

[1] A. L. Demirel and S. Granick, J. Chem. Phys. **115**, 1498 (2001).
[2] D. Y. C. Chen and R. G. Horn, J. Chem. Phys. **83**, 5311 (1985).
[3] Y. Zhu and S. Granick, Phys. Rev. Lett. **87**, 096105 (2001).
[4] Y. Zhu and S. Granick, Phys. Rev. Lett. **88**, 106102 (2002).
[5] A. Slocum, Precision Machine Design, SME, Dearborn, MI, 1992.
[6] U.S. Patent No. 5,964,242 (12 Oct., 1999).
[7] S. Timoshenko, *Theory of Plates and Shells* (McGraw-Hill, New York, 1940).
[8] R. J. Roark, *Formulas for Stress and Strain* (McGraw-Hill, New York, 1943).
[9] J. K. Bhardwaj and H. Ashraf, Proc. SPIE **2639**, 224 (1995).
[10] L. B. Loeb, *The Kinetic Theory of Gases* (Dover, New York, 1961).
[11] J. White, *The Nanogate: Nanoscale Flow Control* (MIT Press, Cambridge, MA, 2003).

Downloaded 11 Oct 2008 to 18.100.0.118. Redistribution subject to AIP license or copyright; see http://rsi.aip.org/rsi/copyright.jsp